Effect of multiple injection strategies on emissions and performance in the Wärtsilä 6L 46 marine engine. A numerical approach

Lamas, Maria Isabel; Rodríguez, Juan de Dios; Castro-Santos, Laura; Carral, Luis Manuel

Universidade da Coruña, Departamento de Enxeñaría Naval e Oceánica, Escola Politécnica Superior, Esteiro, 15403 Ferrol, Spain.

Corresponding author: M. I. Lamas. e-mail: isabellamas@udc.es

ABSTRACT

The present paper proposes a Computational Fluid Dynamics model to analyze the operation cycle and exhaust gas composition in a four-stroke marine diesel engine, the Wärtsilä 6L 46. Once validated, the numerical model was employed to study the influence of several pre-injection parameters such as pre-injection rate, duration, starting instant and number of pre-injections. The purpose is to reduce consumption and emissions, especially nitrogen oxides, due to the current increasingly restrictive legislation. It was found that the fuel injection is a critical factor influencing combustion and emission characteristics. Important nitrogen oxides emission reductions were obtained for the parameters analyzed. Particularly, a 31.9% nitrogen oxides reduction was obtained using 20% pilot injection, 65.7% advancing 4º the pre-injection start angle, 20.1% shorting 4º the pre-injection duration and 36.7% using 4 pre-injections. A slight increment of hydrocarbons, carbon monoxide and consumption was obtained, lower than 5% for almost all the cases analyzed, and a negligible effect on carbon dioxide emissions.

KEYWORDS

Diesel engine, emissions, injection, computational fluid dynamics (CFD).

1- INTRODUCTION

Nowadays, emission reduction in engines is one of the most important challenges that designers are facing, especially nitrogen oxides (NO_x) reduction. Many solutions have been developed in recent years to reduce NO_x emissions. Some methods directly improve combustion such as exhaust gas recirculation, water addition, modification of the injection process, etc. Other methods are based on exhaust gas after treatments, such as selective catalytic reduction systems. Among them, this paper focuses on multiple injection strategies. The first studies about multiple injections in engines appeared in the

nineties. One can refer to the work of Nehmer and Reitz (1998), who studied multiple injection strategies in a heavy duty direct injection diesel engine and obtained reductions in particulate and NO_x emissions, especially if multiple injections are combined with EGR (Exhaust Gas Recirculation). The same conclusion using the same engine was obtained by Han *et al.* (1996) through a numerical model. Using other engines, Ikegami *et al.* (1997) also obtained reductions in particulate and NO_x. Besides, they indicated that another advantage of pilot injections is the reduction of noise. Carlucci *et al.* (2003) analyzed the pilot injection timing and duration and found that NO_x emissions levels are mainly influenced by the pilot duration, whereas smoke emission is influenced by both variables. Mohan *et al.* (2013) reported that post/after injections must be immediately injected after main injection in order to avoid increments in smoke, hydrocarbons (HC) and consumption. Mathivanan *et al.* (2016) indicated that soot can increase because pilot injections aggravate spray characteristics and particulates can be formed at the rich region. Chen (2000) indicated that a high separation between pilot and main injection reduce NOx but long delays might lead to increment smoke, consumption and HC emissions. Minani *et al.* (1995) obtained NO_x reductions but recommended to employ a small amount of pilot quantity in order to maintain soot emissions. Awargal *et al.* (2013) analyzed the time and quantity of the pilot injection, obtaining important NO_x reductions but at expenses of smoke increments. Fang *et al.* (2015) analyzed the effect of the injection angle when using multiple injections, obtaining NO_x reductions but HC increments. Other authors recommend to combine multiple injections with other systems such as EGR, Chen *et al.* (2017), or high injection pressures, Cha *et al.* (2015).

Based on these aforementioned experimental works, it can be concluded that multiple injections are able to reduce emissions but many parameters must be optimized such as injection time, duration of injection, number of pre-injections, dwelling time, etc. In recent years, numerical procedures have become an interesting tool to study injection parameters in engines since it is possible to analyze many solutions avoiding complex and expensive experimental setups. Besides, a numerical model provides interesting information which helps to understand the combustion process and emissions formation. In this regard, Petranovic *et al.* (2015) highlighted the capabilities of CFD (Computational Fluid Dynamics) to decrease the time and cost of experimental researches. Soni *et al.* (2017) developed a numerical model to analyze the effect of the spray angle using two piston bowl geometries. Fajri *et al.* (2017) analyzed numerically the effect of start of combustion, combustion duration, and other parameters on the performance and NO_x emissions. In another numerical work, Nazemi and Shahbakhti (2016) studied the effect of the spray angle, SOI timing, injection pressure and pressure rise rate. Imram *et al.* (2014) analyzed the effect of pilot fuel injection and indicated that an important quantity of NO_x is formed in the region around the pilot spray, where high temperatures exist. Li *et al.* (2016) studied the effect of split injections coupled with swirl and obtained reductions in both consumption and soot emissions. Another numerical analysis was developed by Yu *et al.* (2017), who focused on the injection interval and fuel injection proportion.

This study aims to offer a validated CFD model to provide information about the injection system. Several injection parameters were analyzed such as pre-injection rate, duration, starting instant and number of pre-injections in the marine diesel engine Wärtsilä 6L 46. The goal is to reduce consumption and emissions and provide a cheap and fast tool for studying engines and developing new designs. This work provides a model than can be employed to reduce consumption and emissions in future engines.

2- DEVELOPMENT OF THE MODEL

2.1 Case studied

The engine studied in the present paper, the Wärtsilä 6L 46, is a four-stroke, medium-speed, marine diesel engine with 6 cylinders in line. Each cylinder has two intake and two exhaust valves in the cylinder head. This is a direct injection engine, *i.e.*, the fuel is injected directly into the combustion chamber. A fuel injector is located near the outer edge of the combustion chamber. The nozzle has 10 holes of 0.65 mm diameter and 144º spray angle. Other data of the engine are indicated in Table 1.

Table 1. Specifications of the engine.

Parameter	Value
Output (kW)	5430
Mean effective pressure (kPa)	2250
Speed (rpm)	500
Cylinder displacement volume (cm^3/cyl)	96400
Bore (mm)	460
Stroke (mm)	580

In the present work, an extensive analysis was performed in a Wärtsilä 6L 46 installed on a tuna fishing vessel. Many parameters were characterized at different loads such as in-cylinder pressure, consumption, power, scavenging air pressure and temperature, exhaust gas pressure and temperature, lubricating oil pressure and temperature, cooling water temperature, etc. Although this engine is designed to operate under heavy fuel oil, marine diesel oil operation is also possible. Since these data were taken on board and near the coast, marine diesel oil was employed. The viscosity and density of this fuel are 12.5 mm^2/s and 885 kg/m^3 at 15ºC and its sulfur content 0.89%. The engine operated 2 hours at 25% load, 2 hours at 35%, 2 hours at 50%, 2 hours at 75% and 2 hours at 100% load. 8 tests were taken at each analyzed load and the average was taken. As the engine has 6 cylinders, one test per cylinder was carried out. The engine performance analyzer MALIN 6000 was employed, which is a portable instrument commonly used for preventive maintenance. The pressure transducer included in MALIN 6000 is piezoelectric with 1% accuracy. This is connected to the bleed valve, located at the engine head. The signal from the pressure transducer is processed by a computer. Concentrations of NO_x, CO (carbon monoxide), HC and CO_2 (carbon dioxide) were also analyzed at different loads using the Gasboard-3000 series (Wuhan Cubic) gas analyzers. The accuracy and measurement range of these composition analysis instruments are indicated in Table 2.

Table 2. Accuracy and measurement range of the composition analysis instruments.

Gas	Accuracy	Range
NO$_x$	3%	0-2000 ppm
CO	3%	0-5000 ppm
HC	2%	0-1000 ppm
CO$_2$	2%	0-25%

Some experimental data at different loads are indicated in Table 3. Particularly, the velocity (RPM, revolutions per minute), power, IMEP (indicated mean effective pressure), maximum pressure, SFC (specific fuel consumption) and fractions of NO$_x$, HC, CO and CO$_2$.

Table 3. Experimental data.

Load (%)		25	35	50	75	100
RPM		500	500	500	500	500
Power (kW)		2047.6	2367.8	2923.6	4051.1	5430.1
IMEP (kPa)		810	1390	1760	2000	2250
p$_{max}$ (kPa)		10270	13800	16040	17580	18630
SFC (g/kWh)		173.2	171.9	169.8	169.5	172.1
Fractions	NO$_x$ (ppm)	1048	1092	1149	1167	1128
	HC (ppm)	510	485	448	466	515
	CO (ppm)	261	255	247	268	292
	CO$_2$ (%)	3.5	4.6	6.9	7.9	8.3

2.2 Numerical procedure

The performance cycle of this engine was modeled and validated with experimental results in previous papers (Lamas *et al.*, 2012; Lamas and Rodriguez, 2013; Lamas *et al.*, 2013). The software SolidEdge was employed for the CAD 3D design and Gambit 2.4.6 for the generation of the mesh. The computational mesh is indicated in Fig. 1. As can be seen, the cylinder and valves were meshed. In order to implement the piston movement, a deforming mesh was used and the movement was imposed to the valves and piston surfaces. Particularly, Fig. 1 (a) represents the tridimensional mesh, Fig. 1 (b) a cross-section at BDC (bottom dead center), *i.e.*, 180 or 540º and Fig. 1 (c) a cross-section at TDC (top dead center), *i.e.*, 0º or 360º. The number of elements varied from 50,125 at TDC to 802,527 at BDC. In order to minimize the number of cells and obtain good convergence, hexahedral elements were used to mesh the cylinder. On the other hand, the cylinder head and ducts were meshed using tetrahedrons. In this region the mesh was refined in order to adapt properly to the opening and closing of the valves. Several meshes with different elements were tested in order to verify that the results are independent of the mesh size. Table 4 indicates the error obtained between experimental and numerical results of pressure and fractions using a mesh with 501,769 elements at BDC (mesh 1), as well as 802,527 elements (mesh 2) and 1,264,873 (mesh 3). As can be seen, there is no

difference between the meshes 2 and 3, for this reason the mesh 2 was chosen for the present work.

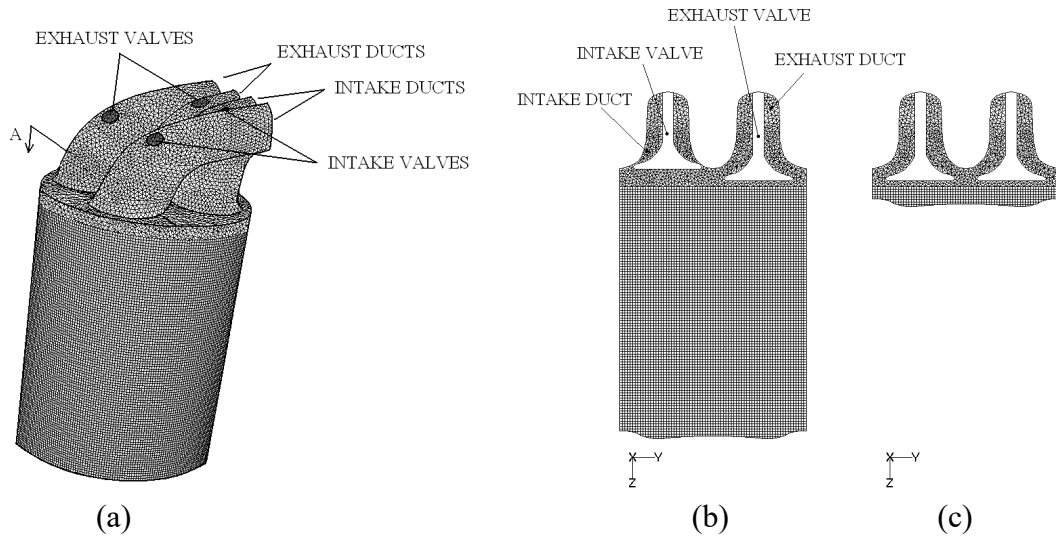(a)   (b)   (c)

Figure 1. (a) Tridimensional mesh at BDC; (b) Cross-section mesh at BDC; (c) Cross-section mesh at TDC.

Table 4. Error (%) at 100% load obtained using different mesh sizes.

	p	NOx	CO	HC	CO2
Mesh 1	4.2	5.1	8.1	6.5	4.7
Mesh 2	4.1	4.9	7.9	6.4	4.6
Mesh 3	4.1	4.9	7.9	6.4	4.6

Regarding the CFD analysis, the open software OpenFOAM was employed because it allows a complete access to the source code in order to modify and program new governing equations which are not implemented by default. A new solver was developed using C++ programming. The governing equations of the present work were programmed from an extension of the solver *dieselEngineFoam*, thereby developing a new CFD solver. A simple backward Euler scheme was used for the temporal treatment, with a constant time step equivalent to 0.1º crank angle. A second order scheme was chosen for discretization of the continuity, momentum, energy and mass fraction equations, and the PISO algorithm was employed for the pressure-velocity coupling.

Basically, the solver is based on the RANS equations of conservation of mass, momentum, and energy. The *k-ε* was employed as turbulence model. The Kelvin-Helmholtz and Rayleigh-Taylor breakup model was used to treat fuel droplet breakup, and the Dukowicz model was applied for the heat-up and evaporation of the droplets. It was assumed that the fuel enters the cylinder as droplets of 10 μm diameter (Challen and Baranescu, 1999; García Oliver, 2006).

The model of Ra and Reitz (2008), based on 41 species and 130 reactions, was employed to characterize the combustion kinetics. The fuel was treated as n-heptane and air as $O_2 + 3.76N_2$. The effect of humidity was neglected.

Fig. 2 represents the CO and HC fractions experimentally and numerically obtained and Fig. 3 the consumption and CO_2 fraction. As can be seen, a reasonable agreement was obtained.
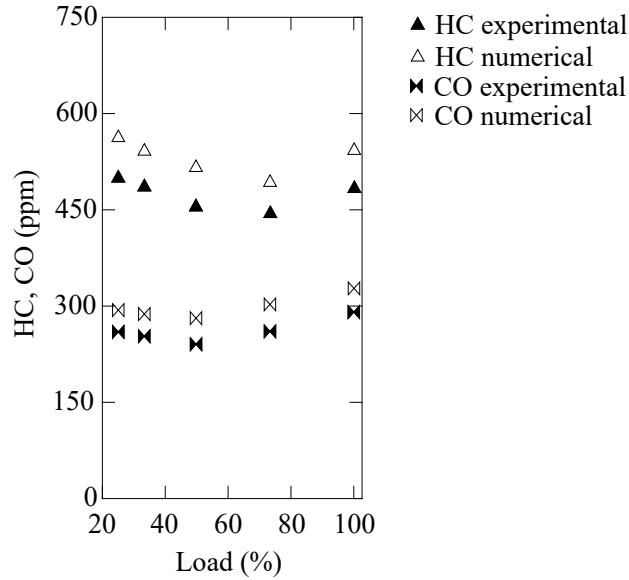

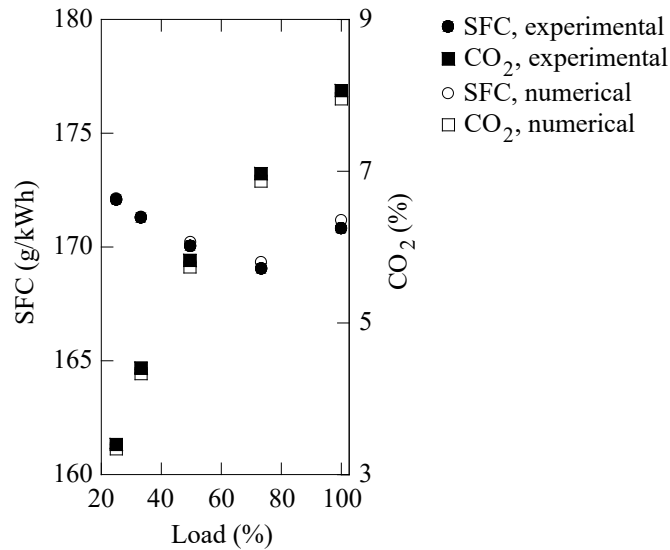Figure 2. HC and CO fractions experimentally and numerically obtained.

Figure 3. SFC and CO_2 fraction experimentally and numerically obtained.

Concerning the kinetics of NO_x, in CFD analysis it is common to employ the extended Zeldovich mechanism, Zeldovich *et al.* (1947) and Lavoie *et al.* (1970), based on the following 3 reactions and 7 species.

$$O+N_2 \leftrightarrow NO+N \tag{1}$$

$$N+O_2 \leftrightarrow NO+O \tag{2}$$

$$N+OH \leftrightarrow NO+H \tag{3}$$

A literature review shows that the extended Zeldovich mechanism, also called thermal mechanism owing to its important temperature sensitivity, provides accurate results for spark ignition engines. Nevertheless, for compression ignition engines the extended Zeldovich mechanism provides a correct NO_x formation trend but it underpredicts NO_x (Aithal, 2010; Rao and Honnery, 2013; Goldsworthy, 2003). Contrary to spark ignition engines, compression ignition engines such diesel or natural gas ones operate under lean conditions, especially if these employ EGR dilution operation. Under lean combustion, the extended Zeldovich mechanism misses some aspects. For instance, N_2O and NNH are important species involved in lean combustion. The main reason is that N_2O and NNH constitute intermediate compounds in the NO formation at relatively low temperatures, while the NO thermal mechanism becomes significant at high temperatures usually higher than 1,400-1,600ºC. Besides, N_2O yields in significant amounts in locally lean, low-temperature regions (Loffler et $al.$, 2006; Hernandez et $al.$, 2006). According to this, a more appropriate chemical mechanism than the extended Zeldovich one is required to predict NO_x formation. Several extended NO_x formation mechanisms have been developed in the literature. For instance, those of Hernández et $al.$ (2008), based on 83 reactions and 38 species; Zabetta et $al.$ (2000), based on 353 reactions and 57 species; Miller et $al.$ (1998), based on 67 reactions and 13 species, etc. Simplified kinetic schemes with less reactions and species can also be found in the literature. Mellor et $al.$ (1998) developed a model based on 6 reactions and 8 species. Zabetta and Kilpinen (2001) simplified the previous model indicating that only 10 reactions and 11 species are important and the results remain practically inalterable. Yang et $al.$ (2003) used 43 reactions and 20 species of a previous model, Miller et $al.$ (1998), and also obtained reasonable results. Other NO_x sources are prompt and fuel. In diesel engines, prompt NO formation is negligible due to the very short residence times in the thin diffusion flames, Heiwood (1988). Fuel NO formation is also negligible due to the low proportion of nitrogen in the fuel.

In order to improve NO_x predictions, in the present paper the extended Zeldovich model was compared to those of Mellor et $al.$ (1998), Zabetta and Kilpinen (2001) and Yang et $al.$ (2003). The results are indicated in Fig. 4. As can be seen, all kinetic schemes provide a correct NO_x trend. The extended Zeldovich model underpredicts the results with a 16.5% error. The other mechanisms also underpredict the results, but provide an error 8.1% corresponding to Mellor et $al.$ (1998), 7.2% Zabetta and Kilpinen (2001) and 4.9% Yang et $al.$ (2003). For this reason, the model of Yang et $al.$ (2003) was chosen for the simulations of the remained of the present paper.
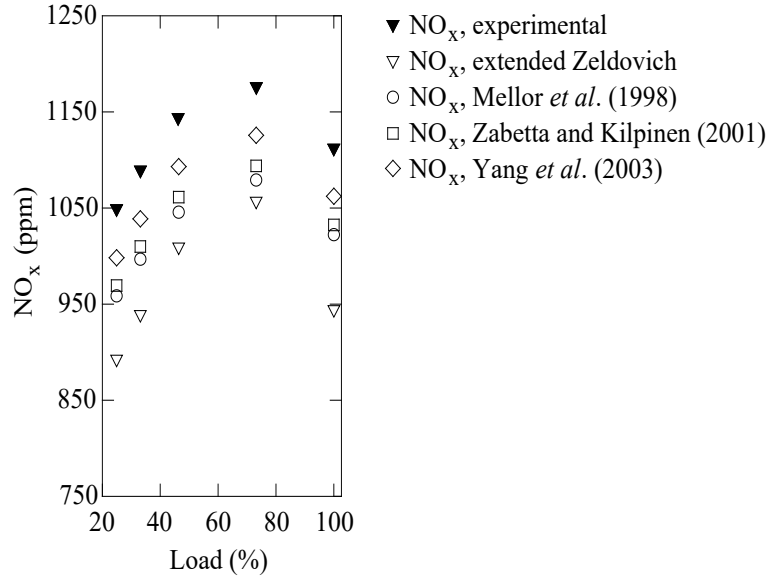
Figure 4. NOₓ fraction experimentally and numerically obtained.

Fig. 5 indicates a comparison between experimentally and numerically obtained in-cylinder pressure for the whole operating cycle at 100% load and the heat release rate from 0 to 180º. The heat release rate was calculated by the following expression, Heywood (1988):

$$\frac{dQ}{d\theta} = \frac{\gamma}{\gamma-1} p \frac{dV}{d\theta} + \frac{1}{\gamma-1} V \frac{dp}{d\theta} \qquad (4)$$

where $dQ/d\theta$ is the heat release rate per crank angle, θ the crank angle, p the in-cylinder pressure, V the in-cylinder volume and γ the polytropic index.
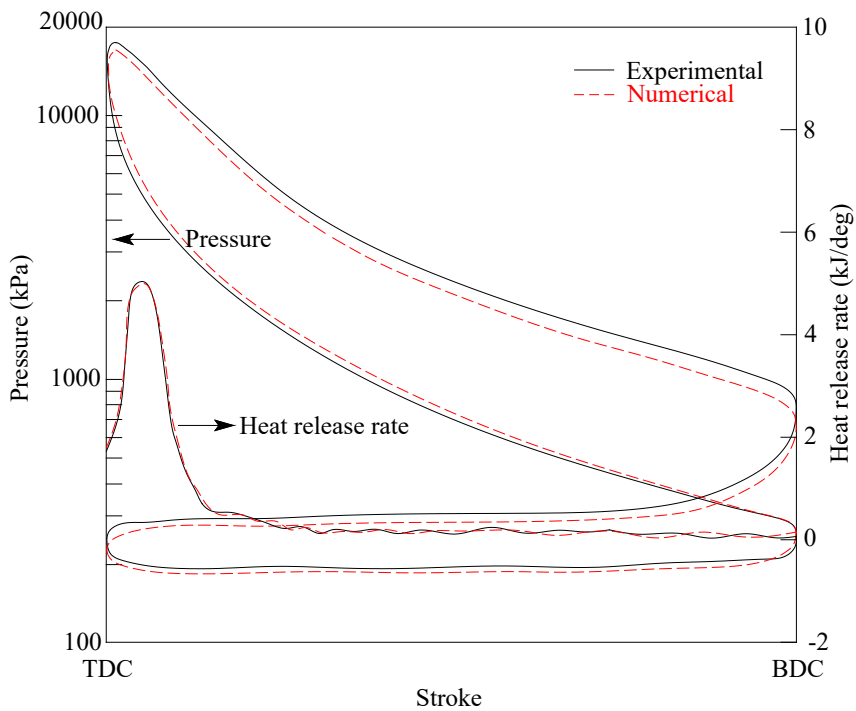
Figure 5. In-cylinder pressure and heat release rate experimentally and numerically obtained at 100% load.

8

Fig. 6 indicates the experimental and numerical mean pressure between -30º and 120º crankshaft angles at 25%, 50% and 100% loads and Fig. 7 indicates the experimental and numerical mean pressure for -90º, -60º, -30º, 0º, 30º, 60º and 90º crankshaft angles and 25%, 35%, 50%, 75% and 100% loads. Regarding fractions, Table 5 indicates the error obtained at different loads. As can be seen, Figures 5-7 and Table 5 indicate that the numerical results are in satisfactory agreement with experimental ones. Several reasons are responsible for the discrepancies between numerical end experimental results. Both numerical techniques and experimental measurements introduce inevitable errors. Experimental errors are associated to the tolerance of the instruments employed and numerical errors are caused by the hypothesis assumed and the discretization processes.
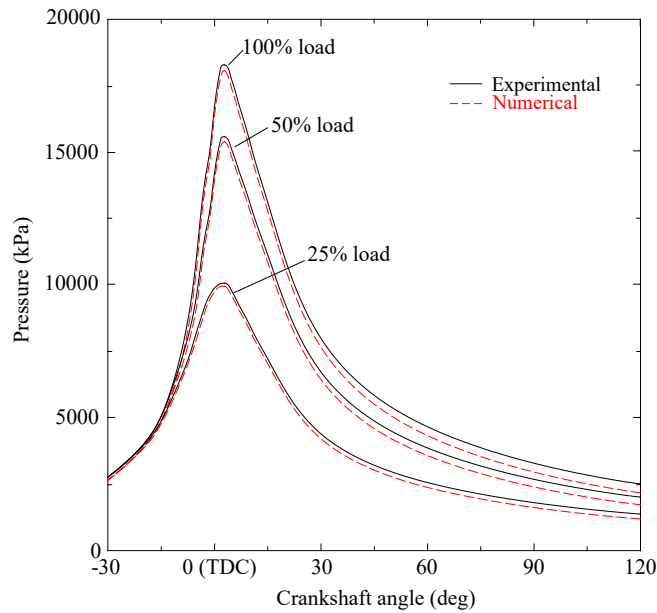

Figure 6. In-cylinder pressure experimentally and numerically obtained at 25%, 50% and 100% loads.
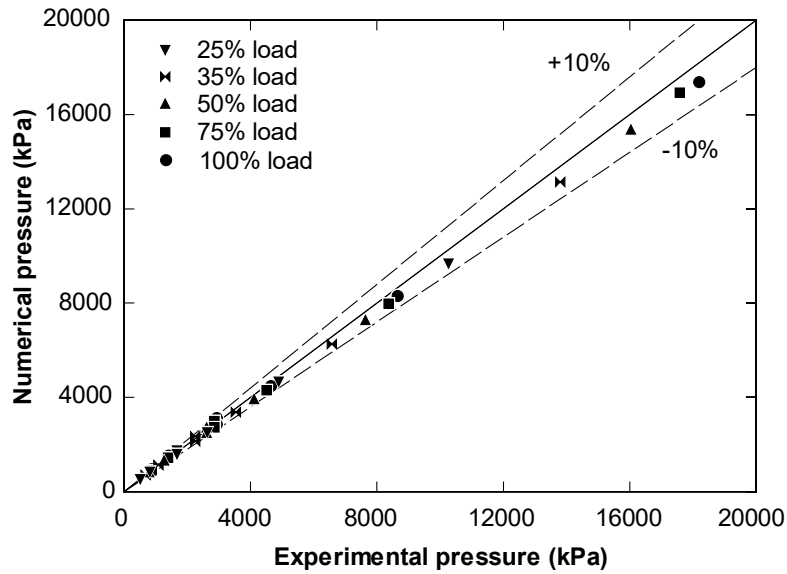
Figure 7. Comparison between in-cylinder pressure experimentally and numerically obtained at different loads.

Table 5. Error (%) in the fractions at different loads.

Load (%)		25	35	50	75	100
Error (%)	NO_x	5.4	5.1	4.5	4.4	4.9
	HC	6.5	6.7	6.9	7.2	6.4
	CO	8.1	8.3	8.5	8.2	7.9
	CO_2	5.2	5.0	4.9	4.8	4.6

3- RESULTS AND DISCUSSION

Once it was validated, the numerical model was employed to study several injection parameters such as pre-injection rate, duration, starting instant and number of pre-injections. The results are indicated below.

In the work of Lamas *et al.* (2012), injection takes place from -12º to -1º. In order to analyze the pre-injection effect, a portion of the combustible was pre-injected from -18º to -14º at 100% load using a constant amount of total fuel per cycle, 9.96 g. The in-cylinder pressure for 10% and 20% pre-injection rates is indicated in Fig. 8. As can be seen, a lower maximum pressure is reached using pre-injection. When pre-injection is employed the combustion process starts earlier and the burn duration increases when compared to the cases without pre-injection. The objective of pre-injection is to limit the initial rate of heat release to keep the maximum pressure at minimum. As lower pressures promote lower temperatures, the NO_x fractions are lower as pre-injection percentage is increased. In this regard, pre-injection is notably different than simply advancing the main injection timing since the former prepares the mixture for the main injection.
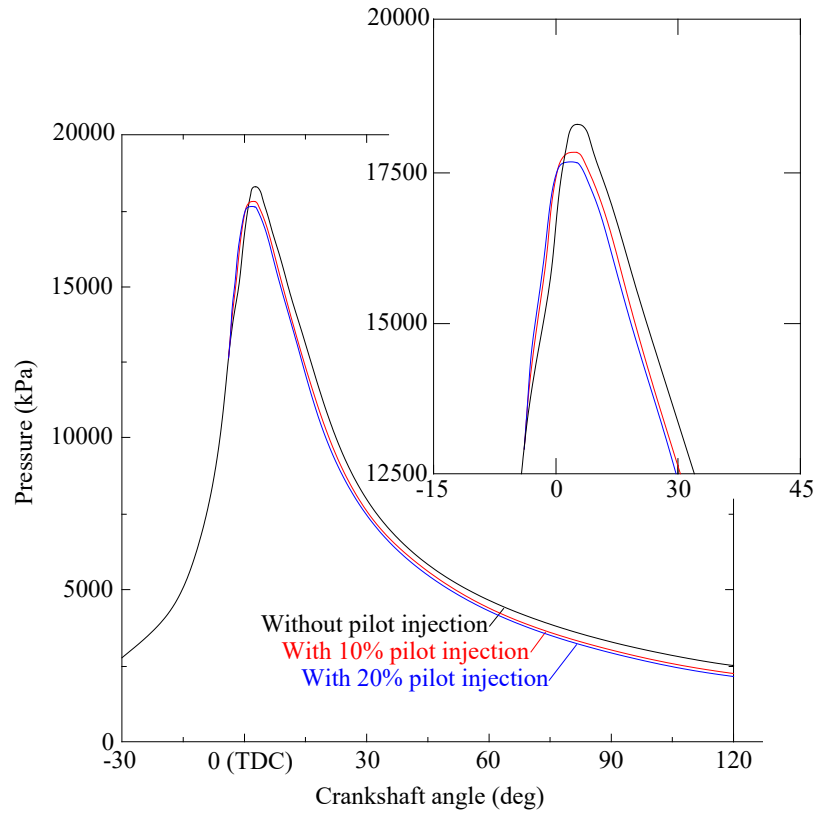
Figure 8. In-cylinder pressure numerically obtained, without pre-injection and with 10% and 20% pre-injection rates.

The average and maximum in-cylinder temperature using 10% and 20% pre-injection rates is indicated in Fig. 9. As can be seen, the temperature is lower using pre-injection. The reduction in NO_x fractions is shown in Fig. 10, which represents the average NO_x against the crankshaft angle using 10% and 20% pre-injection rates. Fig. 11 indicates the NO_x field in the middle cross-section without pilot injection and using 20% pilot injection for 10º and 15º crankshaft angles.
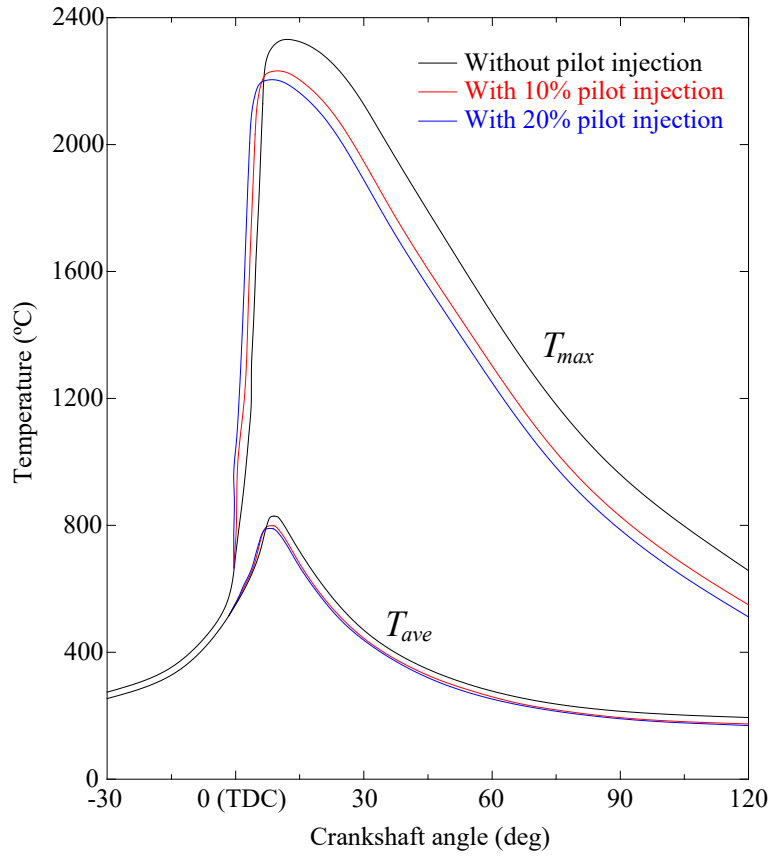
Figure 9. In-cylinder average temperature numerically obtained, without pre-injection
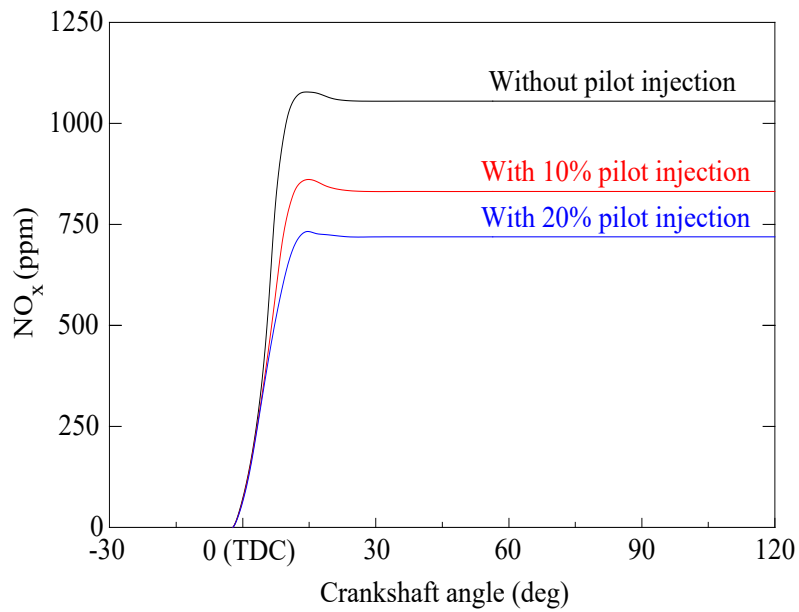and with 10% and 20% pre-injection rates.

Figure 10. NO_x fraction numerically obtained, without pilot injection and with 10% and
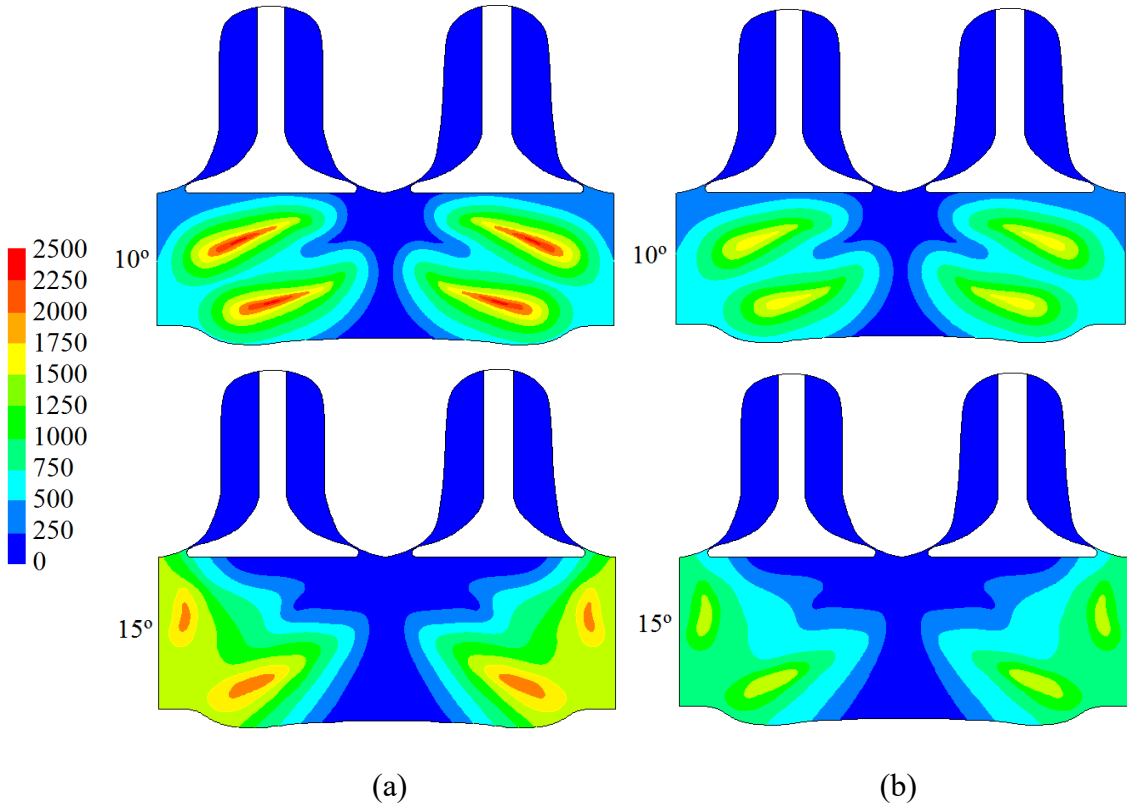20% pilot injection.

Figure 11. NO$_x$ field (ppm); (a) without pilot injection; (b) with 20% pilot injection.

It is interesting to analyze the effect of pre-injection more carefully. Fig. 12 indicates the influence of the pre-injection rate in emissions and consumption for a range between 0% and 20%. This figure indicates emissions in g/kWh. The relation between emissions and gas fractions is provided by the following expression:

$$E_i = 10^6 F_i \frac{M_i}{M_g} \frac{\dot{m}_g}{P}$$

(5)

where E_i is the emission of the component i in g/kWh, F_i the concentration in ppm, M_i the molar mass of the component i, M_g the molar mass of the exhaust gas, $\dot{m}_g$ the exhaust mass flow and P the power.

As can be seen in Fig. 12, consumption increases with the pilot injection rate. The disadvantage of using pre-injection is that this induces lower pressures and thus lower indicated power. If the indicated power is reduced, the specific consumption is increased. This figure also indicates that NO$_x$ emissions are notably reduced, up to 31.9% using 20% pilot injection. The reason is that lower pressures are associated to lower temperatures, and NO$_x$ is mainly produced at high temperatures, Zare *et al.* (2017). Regarding HC and CO emissions, these pollutants are mainly associated to incomplete combustion. Lower temperatures promote slow combustion and partial burning, and thus promote HC and CO formation, Nabi *et al.* (2017). Nevertheless, the effect on HC and CO is practically negligible, less than 5%. Regarding CO$_2$, it remains practically constant since the CO$_2$ concentration in the exhaust gas is much higher than those of NO$_x$, HC and CO and small

modifications of these pollutants do not affect CO_2. In this case, carbon molecules form more HC and CO and thus less CO_2 but this decrement is practically negligible.
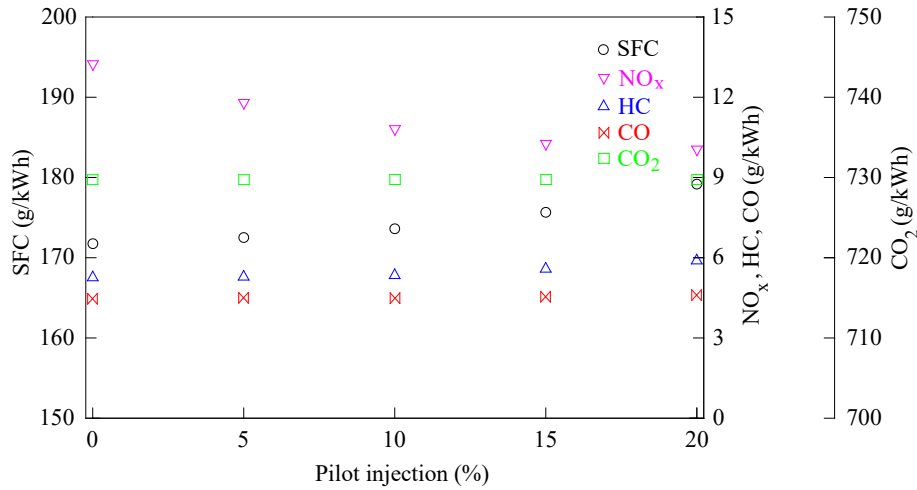

Figure 12. Effect of different pilot injection rates.

Another interesting parameter to study is the pre-injection start angle. Using 10% pre-injection rate and 4º pre-injection duration, the results of different pre-injection start angles are indicated in Fig. 13. As can be seen, NO_x is noticeably reduced when the pre-injection is advanced, up to 65.7% for -22º. Early pilot injections result in more residence time available for the pilot to mix with the surrounding fuel-air mixture, so combustion occurs at locally lean mixtures. Consequently, the local temperatures are lower and thus the tendency to form NO_x. It is important to notice that in practical applications an excessive pre-injection advancement damages the engine because the pressure increment due to combustion must be produced near TDC, when the piston is still moving upward in order to avoid knocking. Another disadvantage of advancing the pre-injection start angle is that lower temperatures promote lower pressures and thus power; consequently, the specific consumption experiments a notably increase. HC and CO are also incremented with pre-injection advancement because lower pressures and thus lower temperatures difficult combustion. CO_2 emissions experiment a practically negligible reduction for the same reason than the previous case.
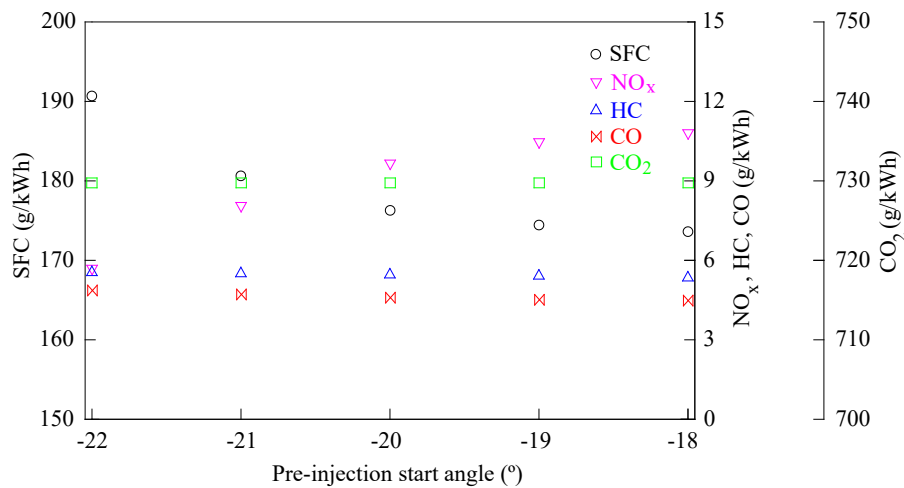

Figure 13. Effect of the pre-injection start angle.

14

The pre-injection duration was also analyzed. Fig. 14 illustrates pre-injection durations between 1º and 5º for 10% pre-injection rate and -18º pre-injection start angle. As can be seen, longer pre-injections increase NO_x emission levels up to 20.1%. The reason is that longer pre-injections make combustion occur closer to TDC and thus produce higher combustion temperatures. Consumption is reduced with the pre-injection duration because higher temperatures are associated to higher pressures and thus higher power. CO and HC emissions decrease with pre-injection duration due to the complete combustion. Besides, large pre-injections involve to inject the combustible slowly and thus the probability to leave non-burnt combustible in form of CO and HC is lower. CO_2 emissions remain practically constant with a slightly increment with pre-injection duration because a more complete combustion promotes that more C is burnt to CO_2 instead CO and HC.
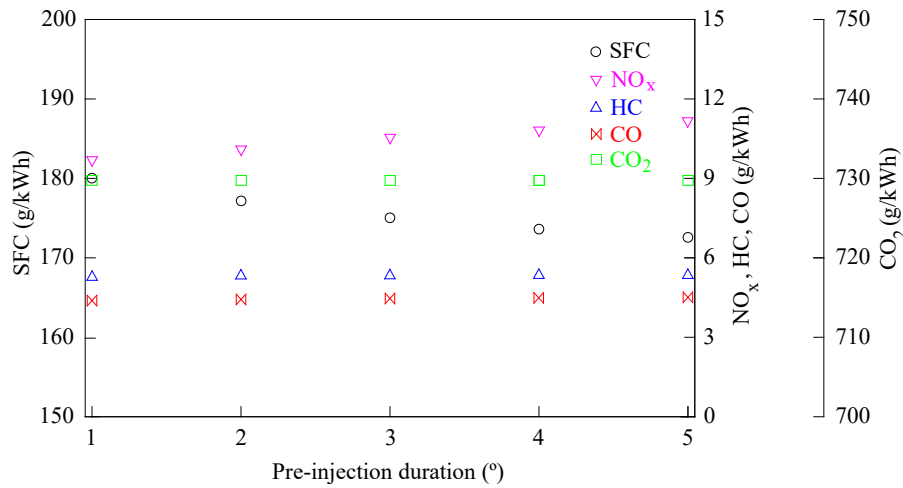

Figure 14. Effect of the pre-injection duration.

Finally, the number of pre-injections was analyzed. Several injections of 2º crankshaft angle duration were analyzed. The results are indicated in Fig. 15. As can be seen, as the number of pre-injections is increased NO_x emissions are reduced up to 36.7%. Pilot injections tend to decrease the size of high-temperature zones and, as a result, NO_x emissions. The specific fuel oil consumption increases with the number of pre-injections due to the lower pressures and thus power. Lower local temperatures promote higher HC and CO emissions, for this reason CO and HC emissions increase with the number of pre-injections. CO_2 emissions remain practically constant with a slightly decrement with the number of pre-injections because more C is employed to form CO and HC instead CO_2.
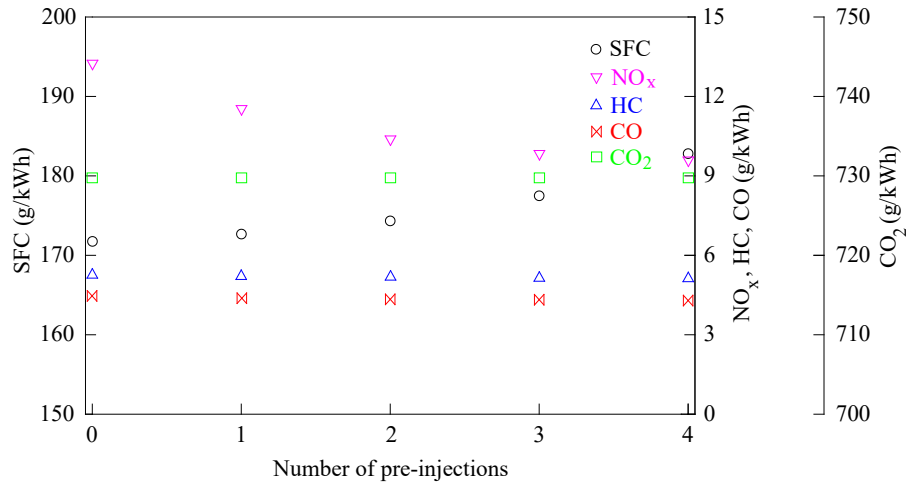
Figure 15. Effect of the number of pre-injections.

Fig. 16 indicates the in-cylinder pressure without pilot injection, using 2 pre-injections and using 4 pre-injections. As can be seen, the maximum pressure is lower as the number of pre-injections is incremented.
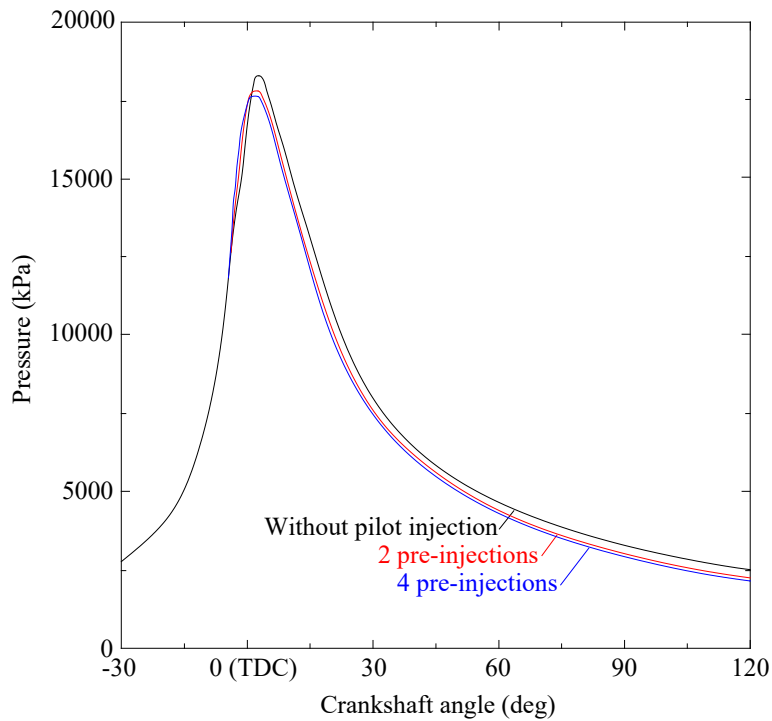

Figure 16. In-cylinder pressure numerically obtained using 2 and 4 pre-injections.

4- CONCLUSIONS

Due to the current necessity to reduce emissions and consumption from engines, the present paper proposes a CFD model to analyze the influence of several injection parameters in a commercial marine diesel engine, the Wärtsilä 6L 46. Experimental measurements were carried out on a Wärtsilä 6L 46 installed on a tuna fishing vessel, and a good agreement between the model and experiments was obtained. NO_x, HC, CO and CO_2 emissions were validated, as well as pressure and consumption. This ensures the accuracy of the present investigation. An open source was employed, OpenFOAM, which is more useful to the scientific community than commercial softwares.

The influence of four injection parameters was analyzed: pre-injection rate, duration, starting instant and number of pre-injections. It was found that NO_x can be noticeably reduced, up to 31.9% if the pre-injection rate is increased to 20%, 65.7% if the pre-injection instant is advanced 4º, 20.1% if the pre-injection rate is shortened 4º and 36.7% if the number of pre-injection rates is increased to four. These measurements, nevertheless, increment CO and HC emissions but this increment resulted less than 5% in most of the cases analyzed. CO_2 emission levels experienced practically negligible modifications.

In future works, the purpose is to apply this model also on two-stroke marine engines used in larger vessels. Once validated, this model can be used to try more modifications and design low emission and consumption engines. This work offers a validated tool very useful to understand the injection parameters and their effect on the combustion and emission process, avoiding laborious and expensive experimental tests.

ACKNOWLEDGEMENTS

NOMENCLATURE

E_i	Emission of the component i (g/kWh)
F_i	Concentration (ppm)
γ	Polytropic index (-)
$\dot{m}_g$	Exhaust mass flow (g/h)
M_g	Molar mass of the exhaust gas (g/mol)
M_i	Molar mass of the component i (g/mol)
θ	Crank angle (deg)
p	In-cylinder pressure (kPa)
P	Power (kW)
Q	Heat released (kJ)
V	In-cylinder volume (m^3)

Abbreviations

BDC   Bottom dead center

CO	Carbon monoxide
CO_2	Carbon dioxide
EGR	Exhaust gas recirculation
HC	Hydrocarbons
IMEP	Indicated mean effective pressure
NO_x	Nitrogen oxides
SFC	Specific fuel consumption
TDC	Top dead center

REFERENCES

Aithal, S.M., 2010. Modeling of NOx formation in diesel engines using finite-rate chemical kinetics. Appl. Energy. 87, 2256-2265.

Awargal, A.K., Dhar, A., Gupta, J.G., Lee, C.S., Park, S., 2013. Effect of fuel injection pressure and injection timing on spray characteristics and particulate size-number distribution in a biodiesel fuelled common rail direct injection system. Appl. Energy. 130, 212-221.

Carlucci, A.P., Ficarella, A., Laforgia, D., 2006. Control of the combustion behaviour in a diesel engine using early injection and gas addition. Appl. Therm. Eng. 26, 2279–86.

Cha, J., Yang, S.H., Naser, N., Ichim, A.I., Chung, S.H., 2015. High pressure and split injection strategies for fuel efficiency and emissions in diesel engine. SAE Tech. Pap. 127084.

Challen, B., Baranescu, R., 1999. Diesel engine reference book. Society of Automotive Engineers.

Chen, G., Wang, K., Yang, J., Zhang, W., Xu, J., Luo, J., 2017. Effects of fuel injection strategy with EGR on diesel engine combustion process and CDPF regeneration performance. Chinese Internal Comb. Engine Eng. 38, 131-141.

Chen, S.K., 2000. Simultaneous reduction of NOx and particulate emissions by using multiple injections in a small diesel engine. SAE Tech. Pap. 2000-01-3084.

Fajri, H.R., Jafari, M.J., Shamekhi, A.H., Jazayeri, S.A., 2017. A numerical investigation of the effects of combustion parameters on the performance of a compression ignition engine toward NOx emission reduction. J. Cleaner Prod. 167, 140-153.

García Oliver, J.M., 2006. The process of direct injection turbulent diesel combustion (in Spanish). Reverté.

Goldsworthy, L., 2003. Reduced kinetics schemes for oxides of nitrogen emissions from a slow-speed marine diesel engine. Ener. Fuel. 17, 450-456.

Han, Z., Uludogan, A., Hampson, G., Reitz, R., 1996. Mechanism of soot and NOx emission reduction using multiple-injection in a diesel engine. SAE Tech. Pap. 960633.

Heywood, J.B., 1988. Internal combustion engine fundamentals. McGraw-Hill.

Hernandez, J.J., Lapuerta, M., Perez-Collado, J., 2006. A combustion kinetic model for estimating diesel engine NOx emissions. Combust. Theor. Model. 10, 639-657.

Hernandez, J.J., Perez-Collado, J., Sanz-Argent, J., 2008 Role of the chemical kinetics on modeling NOx emissions in diesel engines. Ener. Fuel. 22, 262-272.

Ikegami, M., Nakatani, K., Tanaka, S., Yamane, K., 1997. Fuel injection rate shaping and its effect on exhaust emissions in a direct-injection diesel engine using a spool acceleration type injection system. SAE Tech. Pap. 970347.

Imram, S., Emberson, D.R., Ihracska, B., Wen, D.S., Crookes, R.J., Korakianitis, T., 2014. Effect of pilot fuel quantity and type on performance and emissions of natural gas and hydrogen based combustion in a compression ignition engine. Int. J. Hydrogen Energy. 39, 5163-5175.

Lamas, M.I., Rodríguez, C.G., Rebollido, J.M., 2012. Numerical model to study the valve overlap period in the Wärtsilä 6L46 four-stroke marine engine. Polish Marit. Res. 19, 31-37.

Lamas, M.I., Rodríguez, C.G., Rodríguez, J.D., Telmo, J., 2013. Internal modifications to reduce pollutant emissions from marine engines. A numerical approach. J. Nav. Archit. Marine Eng. 5, 493-501.

Lamas, M.I., Rodríguez, C.G., 2013. Numerical model to study the combustion process and emissions in the Wärtsilä 6L 46 four-stroke marine engine. Polish. Marit. Res. 20, 61-66.

Lavoie, G.A., Heywood, J.B., Keck, J.C., 1970. Experimental and theoretical study of nitric oxide formation in internal combustion engines. Comb. Sci. Technol. 1, 313–26.

Li, X., Zhou, H., Zhao, L.M., Su, L., Xu, H., Liu, F., 2016. Effect of split injections coupled with swirl on combustion performance in DI diesel engines. Energy Conv. Manag. 129, 180-188.

Löffler, G., Sieber, R., Harasek, M., Hofbauer, H., Hauss, R., Landaul, J., 2006. NOx formation in natural gas combustion-a new simplified reaction scheme for CFD calculations. Fuel. 85, 513-523.

Mathivanan, K., Mallikarjuna, J.M., Ramesh, A., 2016. Influence of multiple fuel injection strategies on performance and combustion characteristics of a diesel fuelled HCCI engine – An experimental investigation. Exp. Thermal Fluid Sci. 77, 337-346.

Mellor, A.M., 1998. Skeletal mechanism for NOx chemistry in diesel engines. SAE Tech. Pap. 981450.

Miller, R., Davis, G., Lavoie, G., Newman, C., Gardner, T., 1998. A super-extended Zel'dovich mechanism for NOx modeling and engine calibration. SAE Tech. Pap. 980781.

Minami, T., Takeuchi, K., Shimazaki, N., 1995. Reduction of diesel engine NOx using pilot injection. SAE Tech. Pap. 950611.

Mohan, B., Yang, W., Chou, S.K., 2013. Fuel injection strategies for performance improvement and emissions reduction in compression ignition engines. A review. Ren. Sus. Energy Rev. 28, 664-676.

Nabi, M.N., Zare, A., Hossain, F.M., Ristovski, Z.D., Brown, R.J., 2017. Reductions in diesel emissions including PM and PN emissions with diesel-biodiesel blends. J. Cleaner Prod. 166, 860-868.

Nazemi, M., Shahbakhti, M., 2016. Modeling and analysis of fuel injection parameters for combustion and performance of an RCCI engine. Appl. Energy. 165, 135-150.

Nehmer, D.A., Reitz, R.D., 1998. Measurement of effect of injection rate and split injections on diesel engine, soot and NOx emissions. SAE Tech. Pap. 940668.

Petranovic, Z., Vujanovic, M., Duic, N., 2015. Towards a more sustainable transport sector by numerically simulating fuel spray and pollutant formation in diesel engines. J. Cleaner Prod. 88, 272-279.

Ra, Y., Reitz, R., 2008. A reduced chemical kinetic model for IC engine combustion simulations with primary reference fuels. Combust. Flame. 155, 713–738.

Ranz, W.E, Marshall, W.R., 1952. Evaporation from drops - Part 1. Chem. Eng. Prog. 48, 141–8.

Rao, V., Honnery, D., 2013. A comparison of two NOx prediction schemes for use in diesel engine thermodynamic modelling. Fuel. 107, 662-670.

Soni, D., Gupta, R., 2017. Numerical analysis of flow dynamics for two piston bowl designs at different spray angles. J. Cleaner Prod. 149, 723-734.

Yang, H., Krishnan, S.R., Srinivasan, K.K., Midkiff, K.C., 2003. Modeling of NOx emissions using a super-extended Zeldovich mechanism. Proceedings of ICEF03. Fall Technical Conference of the ASME Internal Combustion Engine Division. Erie, Pennsylvania USA.

Yu, H., Liang, X., Shu, G., Wang, Y., Sun, X., Xhang, H., 2017. Numerical investigation of the effect of two-stage injection strategy on combustion and emission characteristics of a diesel engine. Applied Energy. In press.

Zabetta, E.C., Kilpinen, P., Hupa, M., Stähl, K., Leppälahti, J., Cannon, M., Nieminen, J., 2000. Kinetic modeling study on the potential of staged combustion in gas turbines for the reduction of nitrogen oxide emissions from biomass IGCC plants. En. Fuels. 14, 751-761.

Zabetta, E.C., Kilpinen, P., 2001. Improved NOx submodel for in-cylinder CFD simulation of low- and medium-speed compression ignition engines. En. Fuels. 15, 1425-33.

Zeldovich, Y.B., Sadovnikov, D.A., Kamenetskii, F., 1947. Oxidation of nitrogen in combustion. Moscow-Leningrad.

Zare, A., Nabi, M.N., Bodisco, T.A., Hossain, F.M., Rahman, M.M., Van, T.C., Ristovski, Z.D., Brown, R.J., 2017. Diesel engine emissions with oxygenated fuels: A comparative study into cold-start and hot-start operation. J. Cleaner Prod. 162, 997-1008.